Selective Development of Anticorrelated Networks in the Intrinsic Functional Organization of the Human Brain

Citation: Chai, Xiaoqian J., Noa Ofen, John D. E. Gabrieli, and Susan Whitfield-Gabrieli. "Selective Development of Anticorrelated Networks in the Intrinsic Functional Organization of the Human Brain." Journal of Cognitive Neuroscience 26, no. 3 (March 2014): 501-513. © 2014 Massachusetts Institute of Technology

As Published: http://dx.doi.org/10.1162/jocn_a_00517

Publisher: MIT Press

Persistent URL: http://hdl.handle.net/1721.1/85014

Version: Final published version: final published article, as it appeared in a journal, conference proceedings, or other formally published context

Selective Development of Anticorrelated Networks in the Intrinsic Functional Organization of the Human Brain

Xiaoqian J. Chai[1], Noa Ofen[1,2], John D. E. Gabrieli[1], and Susan Whitfield-Gabrieli[1]

Abstract

■ We examined the normal development of intrinsic functional connectivity of the default network (brain regions typically deactivated for attention-demanding tasks) as measured by resting-state fMRI in children, adolescents, and young adults ages 8–24 years. We investigated both positive and negative correlations and employed analysis methods that allowed for valid interpretation of negative correlations and that also minimized the influence of motion artifacts that are often confounds in developmental neuroimaging. As age increased, there were robust developmental increases in negative correlations, including those between medial pFC (MPFC) and dorsolateral pFC (DLPFC) and between lateral parietal cortices and brain regions associated with the dorsal attention network. Between multiple regions, these correlations reversed from being positive in children to negative in adults. Age-related changes in positive correlations within the default network were below statistical threshold after controlling for motion. Given evidence in adults that greater negative correlation between MPFC and DLPFC is associated with superior cognitive performance, the development of an intrinsic anticorrelation between MPFC and DLPFC may be a marker of the large growth of working memory and executive functions that occurs from childhood to young adulthood. ■

INTRODUCTION

Anatomical and functional connections in the human brain mature in a complex and prolonged fashion. White matter pathways mature through young adulthood (Hagmann et al., 2010; Lebel, Walker, Leemans, Phillips, & Beaulieu, 2008; Lenroot & Giedd, 2006). The development of the functional organization of the brain, however, is less well understood. Such development can be investigated using resting-state fMRI (Uddin, Supekar, Ryali, & Menon, 2011; Fair et al., 2007, 2008). In adults, resting-state functional connectivity has revealed that signals in functionally related brain regions correlate with each other in the absence of external stimuli (Beckmann, DeLuca, Devlin, & Smith, 2005; Greicius, Krasnow, Reiss, & Menon, 2003; Biswal, Yetkin, Haughton, & Hyde, 1995). Furthermore, neural networks in the brain are also intrinsically organized into negatively or anticorrelated networks in resting-state fMRI (Fox et al., 2005; Fransson, 2005). Studies of the development of the intrinsic functional organization of the brain have been beset by methodological concerns, including age-associated reductions in movement that can confound analyses (Satterthwaite et al., 2012) and the use of a data preprocessing approach (global signal regression), which mathematically mandates negative correlations and calls into question the interpretation of anticorrelations (Saad et al., 2012; Murphy, Birn, Handwerker, Jones, & Bandettini, 2009). Here, we examined the development of the intrinsic functional organization of the default network, a set of brain regions commonly deactivated during attention-demanding tasks, using methods that minimized these methodological concerns.

We focused on the development of the default network of the brain because it is well defined in adults and because it is related to cognitive functions that grow in development. First, there is a widespread consensus that the default network in adults is consistently comprised of four major regions that exhibit a high degree of correlation during rest, namely the medial pFC (MPFC), the posterior cingulate cortex (PCC), and left and right lateral parietal cortices (LLP and RLP; Raichle et al., 2001). Second, the default network is anticorrelated with task-positive networks, regions commonly activated in tasks that demand attention and mental control (Fox et al., 2005). Third, in adults, the greater degree of resting-state anticorrelation between default and task-positive networks has been linked to superior cognitive control and working memory task performance (Barber, Caffo, Pekar, & Mostofsky, 2013; Hampson, Driesen, Roth, Gore, & Constable, 2010; Kelly, Uddin, Biswal, Castellanos, & Milham, 2008). Given the significant improvement in cognitive control during development (Paz-Alonso, Ghetti, Matlen, Anderson, & Bunge, 2009; Luna, Garver, Urban, Lazar, & Sweeney, 2004; Williams, Ponesse, Schachar, Logan, & Tannock, 1999), we hypothesized that anticorrelations

[1]Massachusetts Institute of Technology, [2]Wayne State University, Detroit, MI

doi:10.1162/jocn_a_00517

between the default and task-positive networks strengthen during development.

Several large-scale functional networks, including the default and attention control networks, have been reported to mature through young adulthood (Barber et al., 2013; Supekar et al., 2010; Supekar, Musen, & Menon, 2009; Fair et al., 2007, 2008). It was proposed that long-range connections strengthen whereas short-range connections weaken during development (Fair et al., 2009; Supekar et al., 2009). Methodological considerations, however, have limited the interpretation of the maturation of correlated and anticorrelated brain regions. Head motion during fMRI is usually highly correlated with age (Satterthwaite et al., 2012), and both head motion and artifacts in functional time series may result in substantial changes in resting-state functional connectivity data despite standard spatial registration and regression of motion estimates (Power, Barnes, Snyder, Schlaggar, & Petersen, 2012; Van Dijk, Sabuncu, & Buckner, 2012). Head motion and artifacts specifically weaken the measurement of long-range connections and strengthen the measurement of short-range connections, which coincides with previously reported developmental changes and raises the concern that some previously reported age-related changes in resting-state connectivity were confounded by motion and artifacts. Furthermore, reports of anticorrelated networks in adults and children have been questioned because global signal regression methods used to identify those networks are known to mathematically generate anticorrelations (Murphy et al., 2009). Prior study of the development of anticorrelated networks has used global signal regression and not employed artifact rejection strategies (Barber et al., 2013). In summary, these methodological concerns make uncertain how the intrinsic functional organization of the default network develops in the human brain.

Here we examined developmental changes in resting-state connectivity of the default network in participants ages 8–24 years. We used methods that minimized the influence of motion artifacts and also allowed for valid identification of anticorrelated networks (Chai, Castanon, Ongur, & Whitfield-Gabrieli, 2012; Whitfield-Gabrieli & Nieto Castanon, 2012; Behzadi, Restom, Liau, & Liu, 2007). We also compared children and adults equated for motion and other artifacts. We tested the hypothesis that anticorrelations between default and task-positives networks increase with age, and we reexamined the development of positive correlations within the default network.

METHODS

Participants

Eighty-two participants (ages 8–24 years, mean age = 14.9 ± 4.4 years, 42 females) were included in the study. There was no age difference between the two genders ($p = .8$). All participants were right-handed, had normal or corrected-to-normal visual acuity, and were screened for history of psychiatric or developmental disorders. The study was approved by the institutional review board of the Massachusetts Institute of Technology. Signed informed consent was obtained before participation. IQ estimates were obtained for each participant based on the KBIT (Second Edition). The mean composite standardized IQ score across participants was 121.5 ± 13.5 (*SD*). Participants' ages and IQ scores did not correlate ($r = .04$, $p = .7$), indicating that participants were cognitively comparable across ages.

Imaging Procedure

Data were acquired on a 3T TrioTim Siemens scanner using a 32-channel head coil. T1-weighted whole-brain anatomical images (MP-RAGE sequence, 256 × 256 voxels, 1 × 1.3-mm in-plane resolution, 1.3-mm slice thickness) were acquired. All participants underwent a resting functional MRI scan of 6.2 min with the instructions "keep your eyes closed and think of nothing in particular." Resting scan images were obtained in 67 2-mm-thick transverse slices, covering the entire brain (interleaved EPI sequence, T2*-weighted images; repetition time = 6 sec, echo time = 30 msec, flip angle = 90°, 67 slices with 2 × 2 × 2 mm voxels). Online prospective acquisition correction (PACE) was applied to the EPI sequence. PACE tracks the head of the subject and updates the position of the field-of-view and slice alignment during acquisition. The parameters for each time point are updated based on motion correction parameters calculated from the previous two time points. Two dummy scans were included at the start of the sequence.

General Image Preprocessing

Resting-state fMRI data were first preprocessed in SPM8 (Wellcome Department of Imaging Neuroscience, London, UK; www.fil.ion.ucl.ac.uk/spm), using standard spatial preprocessing steps. Images were slice-time corrected, realigned and resliced, normalized in MNI space, and smoothed with a 4-mm kernel.

Head Motion and Artifact Detection

Participant head motion, as measured by the mean translation in x, y, z directions (mean = .07 ± .03 mm) decreased with age ($r = .42$, $p < .001$). To address the spurious correlations in resting-state networks caused by head motion, we identified problematic time points during the scan using Artifact Detection Tools (ART, www.nitrc.org/projects/artifact_detect/). Specifically, an image was defined as an outlier (artifact) image if the head displacement in x, y, or z direction was greater than .5 mm from the previous frame, or if the rotational displacement was greater than .02 radians from the previous frame, or if the global mean intensity in the

image was greater than 3 *SD*s from the mean image intensity for the entire resting scan. The number of outlier images (mean = 1.7, max = 14, *SD* = 3.6) decreased with age ($r = -.34$, $p = .002$). At least 4.8 min of non-outlier time points were included in the analysis for each participant. Outlier images were not deleted from the time series, but rather modeled in the first level general linear model (GLM). Therefore, the temporal structure of the data was not disrupted. Each outlier was represented by a single regressor in the GLM, with a 1 sec for the outlier time point and 0 sec elsewhere.

Functional Connectivity Analysis

Functional connectivity analysis was performed using a seed-driven approach with in-house, custom software "CONN" (Chai et al., 2012; Whitfield-Gabrieli & Nieto Castanon, 2012). We included four default network seeds from the MPFC, PCC, LLP, and RLP defined as 10-mm spheres around peak coordinates from the literature (Whitfield-Gabrieli et al., 2009; Fox et al., 2005).

Physiological and other spurious sources of noise were estimated and regressed out using the anatomical CompCor method (aCompCor; Behzadi et al., 2007). Global signal regression, a widely used preprocessing method that mathematically introduces negative correlations (Murphy et al., 2009), was not used. The anatomical image for each participant was segmented into white matter (WM), gray matter, and CSF masks using SPM8. To minimize partial voluming with gray matter, the WM and CSF masks were eroded by one voxel, which resulted in substantially smaller masks than the original segmentations (Chai et al., 2012). The eroded WM and CSF masks were then used as noise ROIs. Signals from the WM and CSF noise ROIs were extracted from the unsmoothed functional volumes to avoid additional risk of contaminating WM and CSF signals with gray matter signals. Previous results showed that aCompCor signals were considerably different from the global signal, as regressing out higher-order principal components of the global signal diminished both positive and negative correlations whereas regressing out aCompCor signals resulted in stronger anticorrelations and eliminated spurious correlations (Chai et al., 2012). On the basis of previous results (Chai et al., 2012), five principal components of the signals from WM and CSF noise ROIs were removed with regression. A temporal band-pass filter of 0.009–0.08 Hz was applied to the time series. Residual head motion parameters (three rotation and three translation parameters, plus another six parameters representing their first-order temporal derivatives) were regressed out. To compare the connectivity maps with or without taking into account the motion artifact outlier images, we ran two separate analyses. In the first analysis, artifactual time points were not regressed out in the model. In the second analysis, each artifact outlier image was included in the model as a separate regressor.

First-level correlation maps were produced by extracting the residual BOLD time course from each seed and computing Pearson's correlation coefficients between that time course and the time course of all other voxels. Correlation coefficients were converted to normally distributed z scores using the Fisher transformation to allow for second-level GLM analyses. To compare with previous results from the literature (Fox et al., 2005), a group level correlation map in adults was produced from the average correlation map of the four seeds in each adult. To examine the age-related changes in connectivity, first-level connectivity maps from each seed for each participant were entered into a group level whole-brain regression analysis with age as a covariate. In all analyses, reported clusters survived a height threshold of uncorrected $p < .001$ and an extent threshold of FWE-corrected $p < .05$ at the cluster level. Regions that showed either increased or decreased connectivity with age were further examined for their connectivity values using one sample t tests in each age group, children (ages 8–12 years, $n = 32$), adolescents (ages 13–17 years, $n = 31$), and adults (ages 18–24 years, $n = 19$). We did not test for between-group differences for these regions because they were defined from the whole-brain regression analysis with age as regions that exhibited significant age effects. In addition, we explored quadratic models of the developmental maturation of the connectivity values in these regions.

Movement- and Artifact-matched Groups

To further address the effect of head motion, we performed additional analyses that directly compared children and adults who were matched on movement and number of artifactual time points (Figure 1). From the original sample of 32 children and 19 adults, 21 children (ages 8–12 years) and 17 adults were included in the movement- and artifact-matched groups. The groups did not differ significantly in mean movement ($p = .52$) or the number of artifactual time points ($p = .34$). Two-sample t tests were performed to directly compare the connectivity maps between children and adults in the movement- and artifact-matched groups.

Group Analyses with Number of Outliers as a Covariate

To account for the difference in degrees of freedom in the first-level GLM (because of difference in number of outliers) across participants, we repeated the whole-brain age regression analysis of all participants by including the number of outliers as an additional covariate.

Global Signal Regression

We performed an additional analysis in which global signal regression was used instead of aCompCor. All

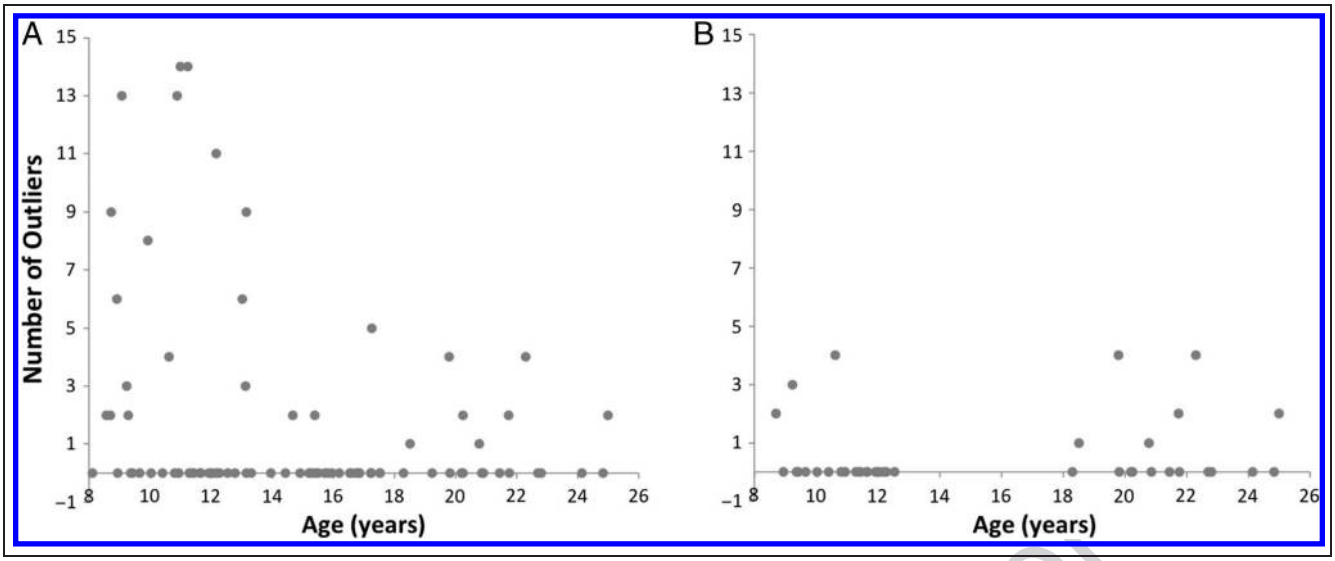

Figure 1. Relation between age and number of outliers in all participants (A) and movement- and artifact-matched groups (B).

the other steps of the analysis streams were identical. After the first-level connectivity maps were created, we performed the same whole-brain regression analysis with age as a covariate as above for each seed.

RESULTS

Default Network and Anticorrelations in Adults

In adults, the mean time course of the four default network seeds was strongly correlated with one another and strongly anticorrelated with regions of previously reported task-positive networks (Fox et al., 2005; Fransson, 2005), including dorsal lateral pFC (BA 46), insular cortex, inferior frontal gyrus (BA 47), and supramarginal gyrus (BA 40; Figure 2). Thus, methods of analysis that allowed interpretation of negative correlations and minimized the influence of motion artifacts support the prior finding of strong positive correlations among the four major nodes of the default network and the strong negative correlations or anticorrelations between the default network and other brain regions often engaged by attention-demanding and working memory tasks.

Developmental Changes of the Default Network Connectivity before and after Artifact Rejection

Because different default network regions might have different developmental patterns, we examined developmental changes in connectivity from each of the four

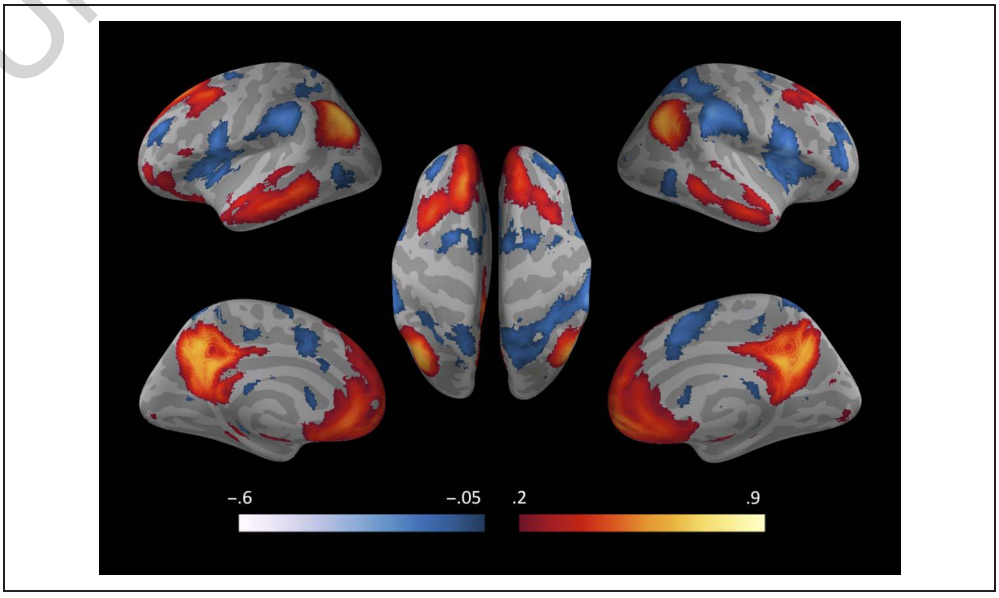

Figure 2. Average correlation map of the four default network seeds in adults. Red represents positive correlations. Blue represents anticorrelations. Correlation values were overlaid on an inflated brain. Left: Lateral and medial views of left hemisphere. Center: Dorsal view. Right: Lateral and medial views of right hemisphere. Color bars represent Pearson's correlation coefficient.

default network seeds in a whole-brain correlation analysis with age (Figure 3). To assess the influence of motion and other artifacts on age-related changes of the resting-state connectivity, we compared two separate analyses in which (1) artifactual time points were not regressed out in the first-level model (pre-ART) and (2) artifactual time points were regressed out in the first-level model (post-ART).

When artifactual time points were not regressed out, we observed increased connectivity with age from the MPFC seed to the other major nodes of the default network (posterior cingulate gyrus and bilateral lateral parietal cortices) during development. However, after artifactual time points were regressed out in the model, no regions showed significant age-related increased connectivity with the MPFC seed during development. At a more liberal threshold ($p < .005$) and without correction, there was a weak correlation with age from the MPFC seed to a region in the posterior cingulate gyrus. The other three seeds (PCC, LLP, and RLP) all showed increased connectivity to the MPFC during development before artifact rejection, but not after artifact rejection. In contrast, many regions that exhibited increased negative connectivity with age (shown in blue in Figure 3) before artifact rejection remained significant after artifact rejection at the same original threshold ($p < .001$, and an extent threshold of FWE-corrected $p < .05$ at the cluster level).

On the basis of these findings and previous reports on the confounding effect of motion and other artifacts on resting-state connectivity development (Power et al., 2012; Satterthwaite et al., 2012), we focused subsequent analyses on the post-ART approach in which artifactual time points were regressed out (Table 1). We further examined the connectivity strengths in regions that showed increasingly negative correlations with age in children, adolescents, and adults.

Development of Anticorrelations of the Default Network

There were robust age-related changes in negative correlations with the default network such that, across the three of the four seeds, there were no significant anticorrelations in children (indeed the correlations were positive instead of negative in many regions), intermediate degrees of anticorrelations in adolescents, and greater and significant anticorrelations in the adults (Figure 4).

Specifically, the MPFC seed was increasingly anticorrelated with the dorsolateral pFC (DLPFC; BA 46, extending through lateral BA 10) across development. Adults, $t(18) = -2.4, p = .03$, and adolescents, $t(30) = -2.5, p = .02$, showed negative correlations between the MPFC and DLPFC, whereas children showed a positive correlation between MPFC and DLPFC, $t(31) = 2.8, p = .008$.

The LLP seed was increasingly anticorrelated with the right supramarginal gyrus, bilateral precuneus, and left FEF across development. Adults showed significant anticorrelations between the LLP and the right supramarginal gyrus, $t(18) = -8.2, p < .001$, bilateral precuneus (left, $t(18) = -3.3, p = .004$; right, $t(18) = -4.3, p < .001$) and FEF, $t(18) = -4.58, p < .001$. Children, in contrast, showed positive correlations with left FEF, $t(31) = 4.8$, $p < .001$, left precuneus, $t(31) = 6.6, p < .001$, and right

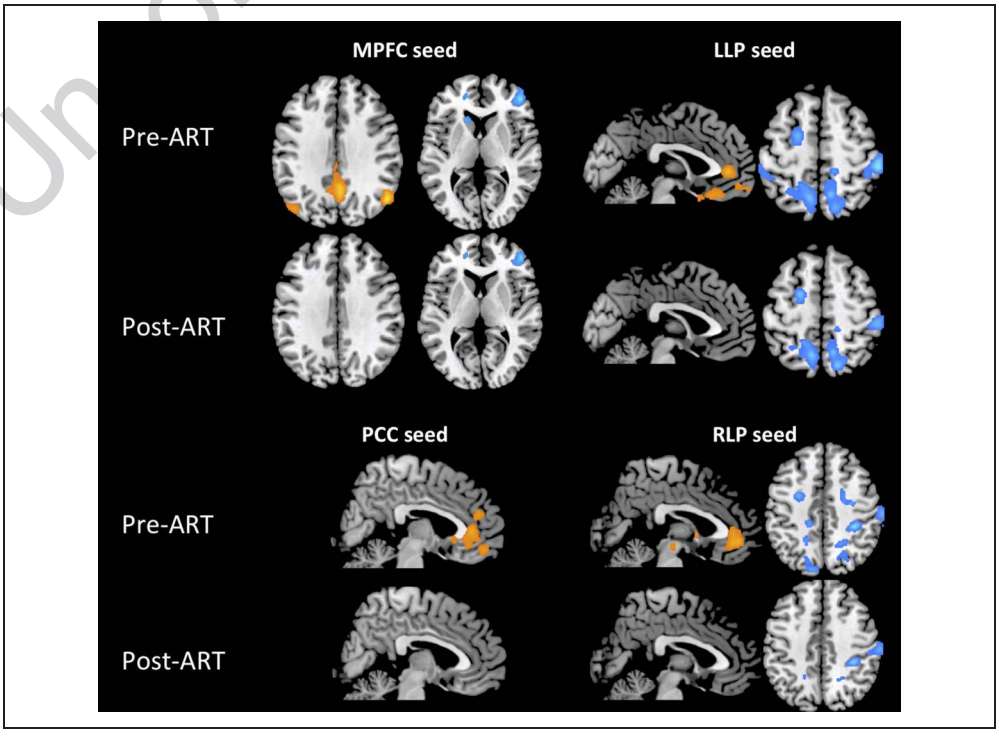

Figure 3. Age-related changes in connectivity with each of the four default network seeds. Regions that showed increased (orange) or decreased (blue) connectivity during development are overlaid on representative brain slices. Age-related changes are shown from analyses before (Pre-ART) and after (Post-ART) artifactual time points were regressed out. Age was entered as continuous variable in the analysis. Axial views: Left side of the image represents left side of the brain.

Table 1. Age-related Changes of Default Network Connectivity (Post-ART)

	BA	*x, y, z*	*T*	*k*
a) MPFC Seed				
Increased correlation with age				
None				
Decreased correlation with age				
R DLPFC	46	46, 42, −2	4.46	156
L anterior pFC	10	−14, 42, −12	4.84	148
R anterior pFC	10	24, 60, −18	4.57	210
b) PCC Seed				
Increased correlation with age				
None				
Decreased correlation with age				
Posterior cingulate gyrus	31	−10, −44, 22	6.65	806
c) LLP Seed				
Increased correlation with age				
L anterior pFC	10	−38, 46, −4	5.70	406
Decreased correlation with age				
R supramarginal gyrus	40	60, −22, 48	5.36	626
L precuneus	7	−10, −65, 51	5.22	1226
R precuneus	7	16, −68, 50	5.25	586
L middle frontal gyrus (FEF)	6	−22, −2, 56	5.03	227
R precuneus	7/31	20, −62, 26	4.43	125
d) RLP Seed				
Increased correlation with age				
Caudate		−10, 0, 0	4.90	154
Decreased correlation with age				
R supramarginal gyrus	40	62, −22, 46	4.86	202
R supramarginal gyrus	40	34, −35, 48	5.40	203
Precuneus	7	16, −68, 66	4.18	215
Precuneus	7/31	−20, −50, 24	5.15	210
Middle temporal gyrus	WM	36, −70, 20	4.61	214

Regions that showed increased or decreased correlation with each of the four default network seeds during development. Age was entered as a continuous variable in the analysis. Artifactual time points were regressed out. Peak coordinates (*x y z*) are based on MNI brain. *k*, cluster size; BA, Brodmann's area.

precuneus, $t(31) = 3.0$, $p = .005$, and no correlation with right supramarginal gyrus. Adolescents showed negative correlations with right supramarginal gyrus, $t(30) = 3.8{,}0$ $p < .001$, positive correlations with left FEF, $t(30) = 2.41$, $p = .02$, and no significant correlation with right precuneus ($p > .2$).

The RLP seed was increasingly anticorrelated with two regions in the right supramarginal gyrus across development. Adults showed significant anticorrelations ($ts < -3.64$, $ps < .002$), whereas children showed positive correlations ($ts > 3.48$, $ps < .002$). Adolescents showed negative correlations with one region in the

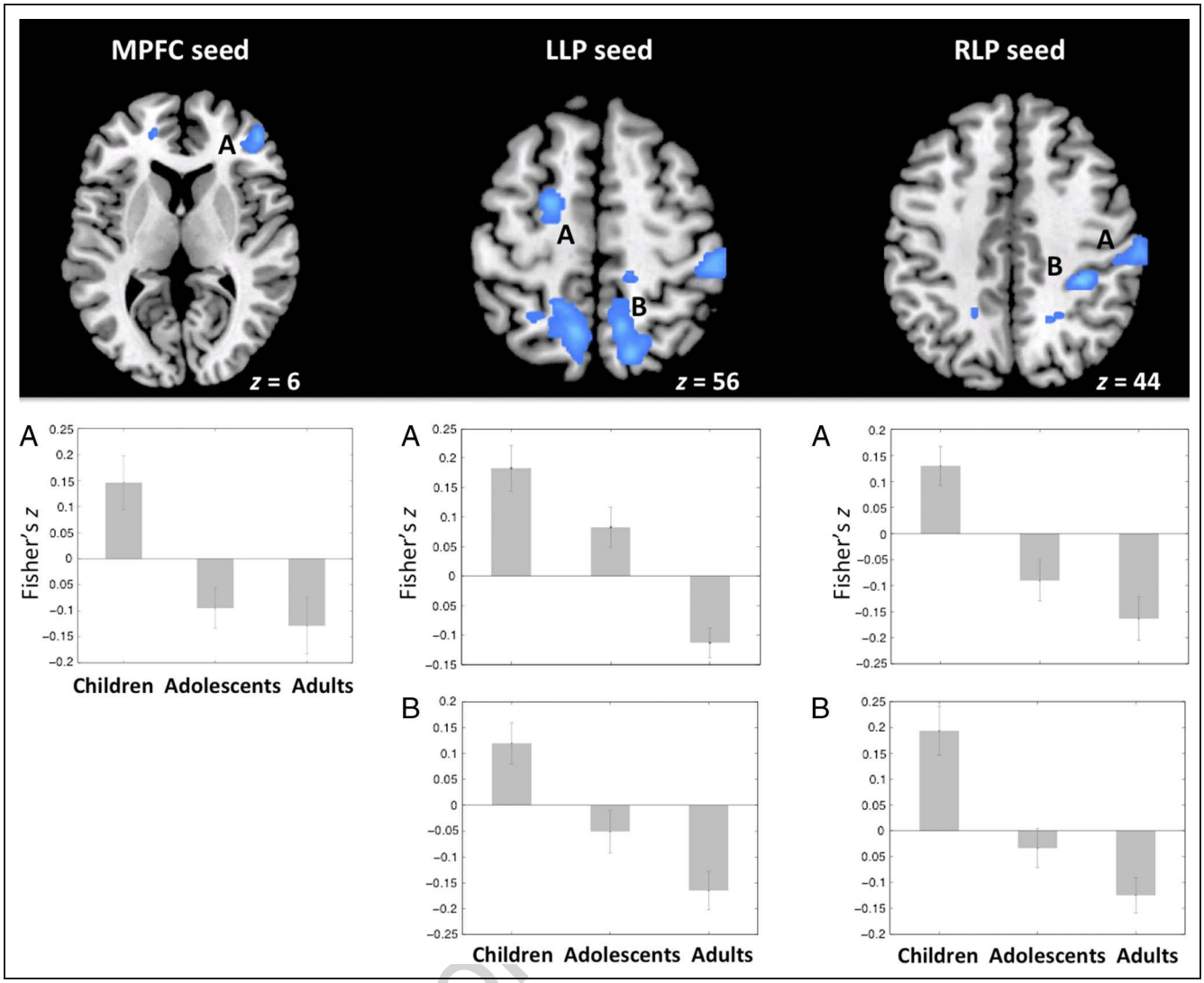

Figure 4. Increased anticorrelations with the default network seeds across development. Connectivity values were extracted from regions that showed decreased correlation with age (as shown in Figure 3) with the MPFC (left), LLP (middle), and RLP (right) seeds. Bar graph represents mean connectivity in three age groups, children (ages 8–12 years, $n = 32$), adolescents (ages 13–17 years, $n = 31$), and adults (ages 18–24 years, $n = 19$). Error bars represent the *SEM*.

right supramarginal gyrus, $t(30) = 2.29$, $p = .03$. We did not observe any developmental change in anticorrelation from the PCC seed.

We repeated the whole-brain age regression analysis after including the number of outliers as a group level covariate. For the LLP seed, there were significant anticorrelation developmental effects in the right supramarginal gyrus and bilateral precuneus at the original threshold. For the MPFC and RLP seeds, the developmental effects were significant at a more liberal threshold of $p < .005$ voxel level uncorrected, $p < .05$ cluster level FWE corrected (MPFC to right DLPFC, and RLP to two regions in the right supramarginal gyrus).

Quadratic Models

There was a quadratic trend ($R^2 = .22$) in anticorrelation growth between MPFC and DLPFC. Anticorrelations between MPFC and DLPFC reached maximum values around 18–20 years and stabilized after that. We did not find quadratic growth trajectory in other anticorrelated regions. We also explored nonlinear models for positive correlations between the MPFC and PCC seeds. There was a weak quadratic trend ($R^2 = .06$), with modest increase from 8 to 16 years and tapering off after that Similarly, we did not find any significant quadratic growth of positive correlations between MPFC and LLP seeds ($R^2 = .12$) or between MPFC and RLP seeds ($R^2 = .04$).

Movement- and Artifact-matched Groups

We directly contrasted the connectivity maps between children and adults who were matched on movement and number of artifactual time points. The findings were similar to those reported above for all children and adults (Figure 5). The MPFC seed was more anticorrelated

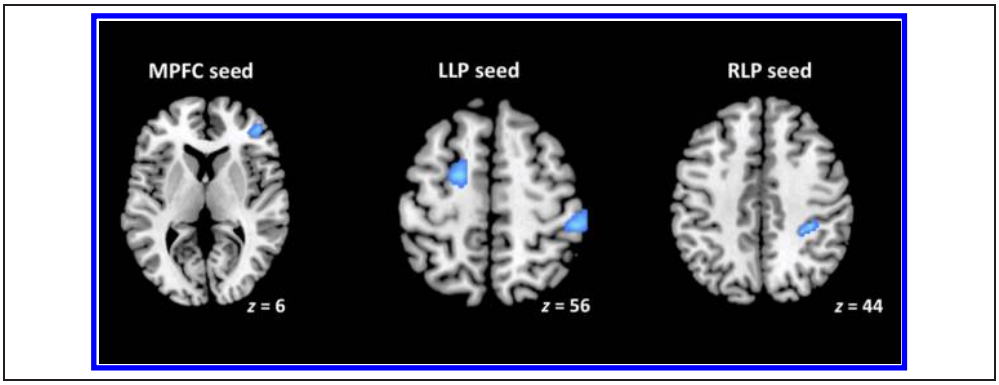

Figure 5. Increased anticorrelations with the default network seeds from children to adults who were matched on motion and artifacts. Shown in blue are regions where adults had significantly greater anticorrelations to default network seeds (MPFC, LLP, and RLP) than did children.

with the DLPFC in adults than children. Adults exhibited a negative correlation, $t(16) = -3.3$, $p = .004$, whereas children exhibited a positive correlation, $t(20) = 4.3$, $p < .001$. The LLP seed again showed more anticorrelation with the right supramarginal gyrus and FEF in adults compared with children. Adults exhibited significant anticorrelations between the LLP and right supramarginal gyrus, $t(16) = -8.4$, $p < .001$, and FEF, $t(16) = 4.2$, $p < .001$, whereas children showed positive correlations between LLP and FEF, $t(20) = 4.2$, $p < .001$. The RLP seed was more anticorrelated with a region in the right supramarginal gyrus in adults compared with children. Adults exhibited significant anticorrelations between the RLP and these two supramarginal gyrus regions, $t(16) = -4.2$, $p < .001$, whereas children exhibited positive correlations, $t(20) = 3.0$, $p = .007$.

The developmental pattern of positive correlations in the matched groups was also similar to results from the regression analysis across all participants above. There was no statistically significant increase in connectivity from the MPFC seed in adults compared with children. No significant developmental changes were observed from the PCC, LLP, and RLP seeds to the MPFC.

Global Signal Regression

When global signal regression was used instead of aCompCor, we did not observe any age-related changes in anticorrelation from any of the four seeds at the original threshold. At a more liberal threshold of $p < .005$ voxel level uncorrected and $p < .05$ cluster level FWE-corrected, one region in the supramarginal gyrus showed an increase in anticorrelation with the LLP seed.

DISCUSSION

Across development from ages 8 to 24 years, there were robust resting-state increases in anticorrelations between the default network and regions in task-positive networks that subserve attention and working memory. The MPFC exhibited increased anticorrelation with the DLPFC during development, whereas the lateral parietal regions exhibited increased anticorrelations with multiple regions of the dorsal attention network that subserves goal-directed attention (Gao & Lin, 2012; Fox, Corbetta, Snyder, Vincent, & Raichle, 2006; Corbetta & Shulman, 2002). The age-related changes in positive correlations within the default network, however, were slight and below statistical threshold after artifactual time points were regressed out.

Analysis of Intrinsic Neural Systems

Compared with previous resting-state fMRI studies in adults and children, this study had three important methodological advances. First, we used an anatomical CompCor (aCompCor) method of noise reduction (Behzadi et al., 2007), as implemented in CONN (Chai et al., 2012; Whitfield-Gabrieli & Nieto Castanon, 2012), which did not involve global signal regression, a widely used preprocessing technique known to mathematically generate uninterpretable anticorrelations (Saad et al., 2012; Wong, Olafsson, Tal, & Liu, 2012; Murphy et al., 2009). Global signal regression was used originally in studies that identified brain regions anticorrelated with the default network (Fox et al., 2005; Fransson, 2005). The present findings with adults identified a similar set of brain regions as being anticorrelated with the default network, showing that under some conditions such global signal regression (despite its biases for negative correlations) does not alter the practical output of analyses. There is accumulating evidence, however, that for developmental research global signal regression may yield misleading outputs. Global signal regression disproportionately alters short- and long-range correlations, which may contribute to spurious group differences between children and adults (Saad et al., 2012). In this study, use of global signal regression eliminated all developmental changes in anticorrelations. The approach used in this study makes negative correlations interpretable and yields higher sensitivity and specificity for positive correlations (Chai et al., 2012). Therefore, increased anticorrelations across development observed in this study should not be because of artifacts from global signal regression but might, instead, have biological validity.

Second, we employed a method of artifact rejection above and beyond motion regression to reduce motion-related artifacts that are common in children. Outlier images in the time series were identified based on both image global intensity and movement criterion and were then statistically removed from subsequent connectivity analyses. Compared with other methods that account for motion using a summary statistic such as the mean movement across the session (e.g., by matching groups on the mean movement or regressing out the mean movement at the group level), this method of artifact rejection has the advantage of accounting for motion artifacts in a scan-to-scan fashion. Similar to previous reports (Power et al., 2012; Satterthwaite et al., 2012), we found that the growth of anterior–posterior correlations in the default network in development was greatly reduced after controlling for head motion. These results highlight the importance of properly controlling for head motion in developmental studies of resting-state connectivity.

Third, we also directly compared children and adults who did not differ significantly in motion and artifact. Therefore, any developmental differences could not be ascribed to issues of interpretation about statistical analyses. The fact that very similar findings were observed for analyses with artifact rejection and analyses for equated groups supports the validity of the analyses that employ artifact rejection.

An additional analytic approach is to include the number of outlier data points as a group level covariate. The pattern of developmental changes was similar, but several age-related changes were less statistically robust. This is likely the consequence of the high correlation between age and movement, such that controlling for movement also minimizes the influence of age.

Development of Anticorrelated Neural Systems

The growth of anticorrelated default and task-positive networks across typical development was consistent and striking. In many regions, children ages 8–12 years exhibited a significantly positive correlation between default and task-positive brain regions, which then became somewhat negatively correlated in adolescents ages 13–17 years and more strongly anticorrelated on adults ages 18–24 years. Thus, typical maturation reversed the intrinsic relations between these brain regions. These reversals of functional brain architecture occurred in cortical regions known to be important for working memory (e.g., DLPFC) and attention (e.g., supramarginal gyrus and FEFs). There have been many imaging studies of the development of working memory and attention, but interpretation of these studies is inevitably complicated by substantial performance differences across ages. The reversal of functional brain architecture cannot be accounted for by such performance differences because they are measured at rest.

A previous developmental study reported age-associated increases in positive default-network correlations in the MPFC, and in negative correlations between the default network and several task-positive regions, including the inferior parietal cortex (BA 40) and precuneus (BA 7; Barber et al., 2013). There are two important methodological differences between Barber et al. (2013) and this study. First, scan-to-scan motion artifacts were not included in the first level analysis in Barber et al. Instead, they compared adults with a group of children with relatively low mean movement across the session and found that the developmental changes in both positive and negative correlations were less robust and extensive in the low-movement group than in the high-movement group. Second, global signal regression was performed in Barber et al., which limited the interpretation of negative correlations (Murphy et al., 2009) and may have introduced spurious group differences (Saad et al., 2012). These methodological differences may have resulted in several differences in findings between our study and Barber et al. (2013). First, we show that the correlations between many regions of DMN and task-positive network reversed from being positive in children to negative in adults, whereas Barber et al. did not show evidence for such a developmental transition. Second, Barber et al. presented results from the averages of three seeds in each network. Our results show that there is considerable heterogeneity among the default network regions in their developmental patterns. Averaging together results from different seeds might reduce the effects that are specific to certain regions. Third, in Barber et al., age-related increase in anticorrelations between DMN and PFC regions (e.g., DLPFC and FEF) were eliminated in the movement-matched groups. Nevertheless, regions that showed increased anticorrelation from Barber et al. (2013) overlapped with a subset of regions found in this study. In general, however, these two studies provide convergent evidence that, over development, the default network and task-positive networks become more inversely coupled.

Studies in infants have examined the development of both correlated and anticorrelated networks. Some studies report that the major nodes of the default network do not develop until 1 and 2 years of age (Fransson, Aden, Blennow, & Lagercrantz, 2011; Smyser et al., 2010; Gao et al., 2009), whereas others report the default network nodes exist at birth (Doria et al., 2010). One study found that anticorrelated networks start to emerge around 2 years (Gao & Lin, 2012); however, global signal regression was implemented in this study. Furthermore, resting-state studies investigating the default network in infants have been done when infants were asleep and may be confounded by the stage of sleep the infants were in when the scanning was performed. It has been shown that during SWS, the MPFC becomes decoupled from the rest of the default network regions (e.g., PCC, LLP, RLP; Horovitz et al., 2009). How different sleep stages interact

with anticorrelation is unknown. Because the current infant literature does not include EEG measurements to determine stages of sleep, interpretations of these studies remain ambiguous.

This study has several limitations. First, we did not have performance measures on working memory or other cognitive control tasks that can be related to the magnitude of anticorrelations during development. Given previous evidence that anticorrelation strengths between the task-positive and the default-mode network are inversely related to executive control performance in adults (Barber et al., 2013; Hampson et al., 2010; Kelly et al., 2008) but not in children (Barber et al., 2013), our results suggest that poor working memory and cognitive control performance in children might be related to the lack of anticorrelations between task-positive network and default network. The second limitation of this study was that we had a repetition time (TR) of 6 sec, which resulted in fewer time points (62 time points, 6.2 min) than most other resting-state fMRI studies. Although this is not ideal, especially because children had more artifactual time points caused by motion, we believe the length of the TR had little influence on the results of our study for two reasons. First, a study showed that there was no significant difference in the correlation strengths between the resting-state networks when compared between a TR of 2.5 and 5 sec (Van Dijk et al., 2010). Second, in our data (Figure 2), we observed characteristic pattern of default network correlation and anticorrelation, which supports the interpretation that the longer TR was not altering the pattern of resting-state connectivity. A third limitation of our study is that it is possible that our modest sample size did not have enough power to detect weaker developmental effects. There is evidence that to reliably detect the developmental increase of connectivity between MPFC and PCC, a sample size of close to 200 participants is required (Satterthwaite et al., 2013). Finally, it may be difficult to completely dissociate brain development from age-correlated decreases in motion artifacts despite the use of multiple methods to mitigate this confound. Matching groups on motion/artifact is probably the best protective measure, but this procedure biases which participants are included in the analysis. The convergence of several analyses, however, supports the view that anticorrelations between the default network and task-positive networks grow with age.

Several lines of evidence from human and animal research support the mathematical and neurophysiological validity of resting-state anticorrelations (Fox, Zhang, Snyder, & Raichle, 2009). Anticorrelated relationships between the default network and executive or attention components of the resting-state networks have been found using alternative approaches such as ICA, which does not involve global signal regression (Cole et al., 2010; Zuo et al., 2010). Also, computational simulations of monkey and human brains suggest existence of spontaneous anticorrelated networks (Deco, Jirsa, McIntosh, Sporns, & Kotter, 2009; Izhikevich & Edelman, 2008; Honey, Kotter, Breakspear, & Sporns, 2007). Finally, the neuronal origins of the anticorrelated fluctuations in the BOLD signals have been explored by electrophysiological studies that found anticorrelated fluctuations of neuronal activity in humans and in cats (Keller et al., 2013; Popa, Popescu, & Pare, 2009).

In adults, the anticorrelation between default and task-positive networks might reflect the fact that during normal, awake behavior, brain activation alternates between networks that support attention to internal thoughts and feeling and other networks that support attention to external stimuli and tasks. During the performance of attention-demanding cognitive control and working memory tasks in healthy adults, greater deactivations of the default network are associated with more demanding performance across conditions or better performance across individuals or trials (Whitfield-Gabrieli et al., 2009; Weissman, Roberts, Visscher, & Woldorff, 2006; Lawrence, Ross, Hoffmann, Garavan, & Stein, 2003; McKiernan, Kaufman, Kucera-Thompson, & Binder, 2003). In parallel, among healthy young adults in the resting state, greater anticorrelations between default and task-positive networks are associated with superior executive and working memory abilities across individuals (Barber et al., 2013; Hampson et al., 2010; Kelly et al., 2008). Furthermore, such anticorrelation appears to be significantly reduced in patient groups with impaired cognitive control, such as patients with schizophrenia (Chai et al., 2011; Whitfield-Gabrieli et al., 2009), attention deficit hyperactivity disorder (Castellanos et al., 2008), bipolar disorder (Chai et al., 2011), Alzheimer's disease (Wang et al., 2007), and altered states of consciousness (Boveroux et al., 2010; Boly et al., 2009). In at least one of these studies (Chai et al., 2011), the patient group did not differ in head motion from the control group; therefore, these differences could not be entirely attributed to motion artifacts. Whether the resting-state anticorrelation is a consequence of effective alternation between brain states during cognitive performance or is also a contributor to such effective alternation is unknown.

A topic of fundamental interest is how the maturation of the brain supports the development of working memory and cognitive control from childhood through adolescence and into young adulthood. This developmental period is characterized by a steep growth in working memory ability and cognitive control (Luna et al., 2004; Kemps, De Rammelaere, & Desmet, 2000). For example, adults, compared with children, are more accurate and have less variability in response time when performing the flanker task, which includes cognitive control over conflicting information (Rueda et al., 2004; Bunge, Dudukovic, Thomason, Vaidya, & Gabrieli, 2002). The growth in working memory ability is associated with functional development of pFC, for example, DLPFC is recruited more by adults than children during working memory and cognitive control tasks (Thomason et al., 2009; Bunge & Wright,

2007; Crone, Wendelken, Donohue, van Leijenhorst, & Bunge, 2006; Bunge et al., 2002). The present findings introduce another development of brain function that may be a marker of the maturation of working memory and cognitive control, namely the growth of intrinsic anti-correlation between the default network and neocortical regions, especially the DLPFC. The increased inverse coupling between regions of the default and task-positive networks across development might be related to better ability to allocate resources between competing internally and externally focused attention and in turn reflect the maturation of cognitive control and executive functions. Future studies that measure both ability in cognitive control and executive functions and also intrinsic functional connectivity in a well-controlled fashion may reveal how strongly these developmental changes are related to one another.

Acknowledgments

The authors thank Christina Triantafyllou for help with imaging protocols; Rebecca Martin, Christiane Mietzsch, Kristina Chambers, Elizabeth Counterman, and Elizabeth Gutierrez for help with data collection; Carlo de los Angeles for help with the manuscript; and the participants and their families. This study was supported by RO1-MH-080344 to J. D. E. G.

Reprint requests should be sent to Dr. Xiaoqian J. Chai, 43 Vassar St., 46-5081, Building 46, Cambridge, MA 02139, or via e-mail: xiaoqian@mit.edu.

REFERENCES

Barber, A. D., Caffo, B. S., Pekar, J. J., & Mostofsky, S. H. (2013). Developmental changes in within- and between-network connectivity between late childhood and adulthood. *Neuropsychologia, 51,* 156–167.

Beckmann, C. F., DeLuca, M., Devlin, J. T., & Smith, S. M. (2005). Investigations into resting-state connectivity using independent component analysis. *Philosophical Transactions of the Royal Society of London, Series B, Biological Sciences, 360,* 1001–1013.

Behzadi, Y., Restom, K., Liau, J., & Liu, T. T. (2007). A component based noise correction method (CompCor) for BOLD and perfusion based fMRI. *Neuroimage, 37,* 90–101.

Biswal, B., Yetkin, F. Z., Haughton, V. M., & Hyde, J. S. (1995). Functional connectivity in the motor cortex of resting human brain using echo-planar MRI. *Magnetic Resonance in Medicine, 34,* 537–541.

Boly, M., Tshibanda, L., Vanhaudenhuyse, A., Noirhomme, Q., Schnakers, C., Ledoux, D., et al. (2009). Functional connectivity in the default network during resting state is preserved in a vegetative but not in a brain dead patient. *Human Brain Mapping, 30,* 2393–2400.

Boveroux, P., Vanhaudenhuyse, A., Bruno, M. A., Noirhomme, Q., Lauwick, S., Luxen, A., et al. (2010). Breakdown of within- and between-network resting state functional magnetic resonance imaging connectivity during propofol-induced loss of consciousness. *Anesthesiology, 113,* 1038–1053.

Bunge, S. A., Dudukovic, N. M., Thomason, M. E., Vaidya, C. J., & Gabrieli, J. D. (2002). Immature frontal lobe contributions to cognitive control in children: Evidence from fMRI. *Neuron, 33,* 301–311.

Bunge, S. A., & Wright, S. B. (2007). Neurodevelopmental changes in working memory and cognitive control. *Current Opinion in Neurobiology, 17,* 243–250.

Castellanos, F. X., Margulies, D. S., Kelly, C., Uddin, L. Q., Ghaffari, M., Kirsch, A., et al. (2008). Cingulate-precuneus interactions: A new locus of dysfunction in adult attention-deficit/hyperactivity disorder. *Biological Psychiatry, 63,* 332–337.

Chai, X. J., Castanon, A. N., Ongur, D., & Whitfield-Gabrieli, S. (2012). Anticorrelations in resting state networks without global signal regression. *Neuroimage, 59,* 1420–1428.

Chai, X. J., Whitfield-Gabrieli, S., Shinn, A. K., Gabrieli, J. D., Nieto Castanon, A., McCarthy, J. M., et al. (2011). Abnormal medial prefrontal cortex resting-state connectivity in bipolar disorder and schizophrenia. *Neuropsychopharmacology, 36,* 2009–2017.

Cole, D. M., Beckmann, C. F., Long, C. J., Matthews, P. M., Durcan, M. J., & Beaver, J. D. (2010). Nicotine replacement in abstinent smokers improves cognitive withdrawal symptoms with modulation of resting brain network dynamics. *Neuroimage, 52,* 590–599.

Corbetta, M., & Shulman, G. L. (2002). Control of goal-directed and stimulus-driven attention in the brain. *Nature Reviews Neuroscience, 3,* 201–215.

Crone, E. A., Wendelken, C., Donohue, S., van Leijenhorst, L., & Bunge, S. A. (2006). Neurocognitive development of the ability to manipulate information in working memory. *Proceedings of the National Academy of Sciences, U.S.A., 103,* 9315–9320.

Deco, G., Jirsa, V., McIntosh, A. R., Sporns, O., & Kotter, R. (2009). Key role of coupling, delay, and noise in resting brain fluctuations. *Proceedings of the National Academy of Sciences, U.S.A., 106,* 10302–10307.

Doria, V., Beckmann, C. F., Arichi, T., Merchant, N., Groppo, M., Turkheimer, F. E., et al. (2010). Emergence of resting state networks in the preterm human brain. *Proceedings of the National Academy of Sciences, U.S.A., 107,* 20015–20020.

Fair, D. A., Cohen, A. L., Dosenbach, N. U., Church, J. A., Miezin, F. M., Barch, D. M., et al. (2008). The maturing architecture of the brain's default network. *Proceedings of the National Academy of Sciences, U.S.A., 105,* 4028–4032.

Fair, D. A., Cohen, A. L., Power, J. D., Dosenbach, N. U., Church, J. A., Miezin, F. M., et al. (2009). Functional brain networks develop from a "local to distributed" organization. *PLOS Computational Biology, 5,* e1000381.

Fair, D. A., Dosenbach, N. U., Church, J. A., Cohen, A. L., Brahmbhatt, S., Miezin, F. M., et al. (2007). Development of distinct control networks through segregation and integration. *Proceedings of the National Academy of Sciences, U.S.A., 104,* 13507–13512.

Fox, M. D., Corbetta, M., Snyder, A. Z., Vincent, J. L., & Raichle, M. E. (2006). Spontaneous neuronal activity distinguishes human dorsal and ventral attention systems. *Proceedings of the National Academy of Sciences, U.S.A., 103,* 10046–10051.

Fox, M. D., Snyder, A. Z., Vincent, J. L., Corbetta, M., Van Essen, D. C., & Raichle, M. E. (2005). The human brain is intrinsically organized into dynamic, anticorrelated functional networks. *Proceedings of the National Academy of Sciences, U.S.A., 102,* 9673–9678.

Fox, M. D., Zhang, D., Snyder, A. Z., & Raichle, M. E. (2009). The global signal and observed anticorrelated resting state brain networks. *Journal of Neurophysiology, 101,* 3270–3283.

Fransson, P. (2005). Spontaneous low-frequency BOLD signal fluctuations: An fMRI investigation of the resting-state default mode of brain function hypothesis. *Human Brain Mapping, 26,* 15–29.

Fransson, P., Aden, U., Blennow, M., & Lagercrantz, H. (2011). The functional architecture of the infant brain as revealed by resting-state fMRI. *Cerebral Cortex, 21,* 145–154.

Gao, W., & Lin, W. (2012). Frontal parietal control network regulates the anti-correlated default and dorsal attention networks. *Human Brain Mapping, 33,* 192–202.

Gao, W., Zhu, H., Giovanello, K. S., Smith, J. K., Shen, D., Gilmore, J. H., et al. (2009). Evidence on the emergence of the brain's default network from 2-week-old to 2-year-old healthy pediatric subjects. *Proceedings of the National Academy of Sciences, U.S.A., 106,* 6790–6795.

Greicius, M. D., Krasnow, B., Reiss, A. L., & Menon, V. (2003). Functional connectivity in the resting brain: A network analysis of the default mode hypothesis. *Proceedings of the National Academy of Sciences, U.S.A., 100,* 253–258.

Hagmann, P., Sporns, O., Madan, N., Cammoun, L., Pienaar, R., Wedeen, V. J., et al. (2010). White matter maturation reshapes structural connectivity in the late developing human brain. *Proceedings of the National Academy of Sciences, U.S.A., 107,* 19067–19072.

Hampson, M., Driesen, N., Roth, J. K., Gore, J. C., & Constable, R. T. (2010). Functional connectivity between task-positive and task-negative brain areas and its relation to working memory performance. *Magnetic Resonance Imaging, 28,* 1051–1057.

Honey, C. J., Kotter, R., Breakspear, M., & Sporns, O. (2007). Network structure of cerebral cortex shapes functional connectivity on multiple time scales. *Proceedings of the National Academy of Sciences, U.S.A., 104,* 10240–10245.

Horovitz, S. G., Braun, A. R., Carr, W. S., Picchioni, D., Balkin, T. J., Fukunaga, M., et al. (2009). Decoupling of the brain's default mode network during deep sleep. *Proceedings of the National Academy of Sciences, U.S.A., 106,* 11376–11381.

Izhikevich, E. M., & Edelman, G. M. (2008). Large-scale model of mammalian thalamocortical systems. *Proceedings of the National Academy of Sciences, U.S.A., 105,* 3593–3598.

Keller, C. J., Bickel, S., Honey, C. J., Groppe, D. M., Entz, L., Craddock, R. C., et al. (2013). Neurophysiological investigation of spontaneous correlated and anticorrelated fluctuations of the BOLD signal. *Journal of Neuroscience, 33,* 6333–6342.

Kelly, A. M., Uddin, L. Q., Biswal, B. B., Castellanos, F. X., & Milham, M. P. (2008). Competition between functional brain networks mediates behavioral variability. *Neuroimage, 39,* 527–537.

Kemps, E., De Rammelaere, S., & Desmet, T. (2000). The development of working memory: Exploring the complementarity of two models. *Journal of Experimental Child Psychology, 77,* 89–109.

Lawrence, N. S., Ross, T. J., Hoffmann, R., Garavan, H., & Stein, E. A. (2003). Multiple neuronal networks mediate sustained attention. *Journal of Cognitive Neuroscience, 15,* 1028–1038.

Lebel, C., Walker, L., Leemans, A., Phillips, L., & Beaulieu, C. (2008). Microstructural maturation of the human brain from childhood to adulthood. *Neuroimage, 40,* 1044–1055.

Lenroot, R. K., & Giedd, J. N. (2006). Brain development in children and adolescents: Insights from anatomical magnetic resonance imaging. *Neuroscience and Biobehavioral Reviews, 30,* 718–729.

Luna, B., Garver, K. E., Urban, T. A., Lazar, N. A., & Sweeney, J. A. (2004). Maturation of cognitive processes from late childhood to adulthood. *Child Development, 75,* 1357–1372.

McKiernan, K. A., Kaufman, J. N., Kucera-Thompson, J., & Binder, J. R. (2003). A parametric manipulation of factors affecting task-induced deactivation in functional neuroimaging. *Journal of Cognitive Neuroscience, 15,* 394–408.

Murphy, K., Birn, R. M., Handwerker, D. A., Jones, T. B., & Bandettini, P. A. (2009). The impact of global signal regression on resting state correlations: Are anti-correlated networks introduced? *Neuroimage, 44,* 893–905.

Paz-Alonso, P. M., Ghetti, S., Matlen, B. J., Anderson, M. C., & Bunge, S. A. (2009). Memory suppression is an active process that improves over childhood. *Frontiers in Human Neuroscience, 3,* 24.

Popa, D., Popescu, A. T., & Pare, D. (2009). Contrasting activity profile of two distributed cortical networks as a function of attentional demands. *Journal of Neuroscience, 29,* 1191–1201.

Power, J. D., Barnes, K. A., Snyder, A. Z., Schlaggar, B. L., & Petersen, S. E. (2012). Spurious but systematic correlations in functional connectivity MRI networks arise from subject motion. *Neuroimage, 59,* 2142–2154.

Raichle, M. E., MacLeod, A. M., Snyder, A. Z., Powers, W. J., Gusnard, D. A., & Shulman, G. L. (2001). A default mode of brain function. *Proceedings of the National Academy of Sciences, U.S.A., 98,* 676–682.

Rueda, M. R., Fan, J., McCandliss, B. D., Halparin, J. D., Gruber, D. B., Lercari, L. P., et al. (2004). Development of attentional networks in childhood. *Neuropsychologia, 42,* 1029–1040.

Saad, Z. S., Gotts, S. J., Murphy, K., Chen, G., Jo, H. J., Martin, A., et al. (2012). Trouble at rest: How correlation patterns and group differences become distorted after global signal regression. *Brain Connectivity, 2,* 25–32.

Satterthwaite, T. D., Wolf, D. H., Loughead, J., Ruparel, K., Elliott, M. A., Hakonarson, H., et al. (2012). Impact of in-scanner head motion on multiple measures of functional connectivity: Relevance for studies of neurodevelopment in youth. *Neuroimage, 60,* 623–632.

Satterthwaite, T. D., Wolf, D. H., Ruparel, K., Erus, G., Elliott, M. A., Eickhoff, S. B., et al. (2013). Heterogeneous impact of motion on fundamental patterns of developmental changes in functional connectivity during youth. *Neuroimage, 83C,* 45–57.

Smyser, C. D., Inder, T. E., Shimony, J. S., Hill, J. E., Degnan, A. J., Snyder, A. Z., et al. (2010). Longitudinal analysis of neural network development in preterm infants. *Cerebral Cortex, 20,* 2852–2862.

Supekar, K., Musen, M., & Menon, V. (2009). Development of large-scale functional brain networks in children. *PLOS Biology, 7,* e1000157.

Supekar, K., Uddin, L. Q., Prater, K., Amin, H., Greicius, M. D., & Menon, V. (2010). Development of functional and structural connectivity within the default mode network in young children. *Neuroimage, 52,* 290–301.

Thomason, M. E., Race, E., Burrows, B., Whitfield-Gabrieli, S., Glover, G. H., & Gabrieli, J. D. (2009). Development of spatial and verbal working memory capacity in the human brain. *Journal of Cognitive Neuroscience, 21,* 316–332.

Uddin, L. Q., Supekar, K. S., Ryali, S., & Menon, V. (2011). Dynamic reconfiguration of structural and functional connectivity across core neurocognitive brain networks with development. *Journal of Neuroscience, 31,* 18578–18589.

Van Dijk, K. R., Hedden, T., Venkataraman, A., Evans, K. C., Lazar, S. W., & Buckner, R. L. (2010). Intrinsic functional connectivity as a tool for human connectomics: Theory, properties, and optimization. *Journal of Neurophysiology, 103,* 297–321.

Van Dijk, K. R., Sabuncu, M. R., & Buckner, R. L. (2012). The influence of head motion on intrinsic functional connectivity MRI. *Neuroimage, 59,* 431–438.

Wang, K., Liang, M., Wang, L., Tian, L., Zhang, X., Li, K., et al. (2007). Altered functional connectivity in early Alzheimer's

disease: A resting-state fMRI study. *Human Brain Mapping, 28,* 967–978.
Weissman, D. H., Roberts, K. C., Visscher, K. M., & Woldorff, M. G. (2006). The neural bases of momentary lapses in attention. *Nature Neuroscience, 9,* 971–978.
Whitfield-Gabrieli, S., & Nieto Castanon, A. (2012). Conn: A functional connectivity toolbox for correlated and anticorrelated brain networks. *Brain Connectivity*.
Whitfield-Gabrieli, S., Thermenos, H. W., Milanovic, S., Tsuang, M. T., Faraone, S. V., McCarley, R. W., et al. (2009). Hyperactivity and hyperconnectivity of the default network in schizophrenia and in first-degree relatives of persons with schizophrenia. *Proceedings of the National Academy of Sciences, U.S.A., 106,* 1279–1284.
Williams, B. R., Ponesse, J. S., Schachar, R. J., Logan, G. D., & Tannock, R. (1999). Development of inhibitory control across the life span. *Developmental Psychology, 35,* 205–213.
Wong, C. W., Olafsson, V., Tal, O., & Liu, T. T. (2012). Anti-correlated networks, global signal regression, and the effects of caffeine in resting-state functional MRI. *Neuroimage, 63,* 356–364.
Zuo, X. N., Di Martino, A., Kelly, C., Shehzad, Z. E., Gee, D. G., Klein, D. F., et al. (2010). The oscillating brain: Complex and reliable. *Neuroimage, 49,* 1432–1445.